THE ASTROPHYSICAL JOURNAL, 408:446–451, 1993 May 10

VLBI OBSERVATIONS OF A COMPLETE SAMPLE OF RADIO GALAXIES. III. THE TWO-SIDED MILLIARCSECOND STRUCTURE OF 3C 338

L. FERETTI,[1,2] G. COMORETTO,[3] G. GIOVANNINI,[1,2] T. VENTURI,[1] AND A. E. WEHRLE[4]
Received 1992 January 16; accepted 1992 November 2

ABSTRACT

We present VLBI and VLA observations of the Fanaroff-Riley "type I" radio galaxy 3C 338. On both milliarcsec and arcsecond scales, the source is characterized by emission on both sides of the core. In the VLBI images, the symmetric structures have three or four "knots" in the emission on each side of the core. The reliability of the VLBI images was extensively tested using two different data reduction procedures.

Detection of equally bright emission on both sides of a parcsec-scale core implies that Doppler boosting is small: either the source orientation is near the plane of the sky, or the twin jets are not highly relativistic. Another possibility is that the jet is intrinsically one-sided and alternately feeds energy into opposite directions.

Subject headings: galaxies: individual (3C 338) — galaxies: jets — techniques: interferometric

1. INTRODUCTION

Radio galaxies of high and low luminosity have quite different radio morphologies on kiloparsec scale. It is not clear how much of this distinction is due to effects arising in the central engine and how much to environmental influences on the propagation of the jets. It is therefore important to look for distinctions on the parsec scale. On parsec scales, the high-luminosity radio galaxies share a common morphology: a compact *core* with one-sided jet extending in the direction of the large-scale jet. In most cases, the cores are known to have flat spectra, like those of radio-loud quasars. Most of the radio galaxy cores that have been mapped with VLBI are high-luminosity objects classed as "FRII" ($L_{178\,\mathrm{MHz}} > 2 \times 10^{25}$ W Hz^{-1} sr^{-1}; Fanaroff & Riley 1974). They can be observed with the easily available Mark II technique (Cohen et al. 1975). Observing FRIs is more difficult: the brightest objects have been mapped first, introducing a selection effect which may mask differencies between the high- and low-luminosity objects. The best studied sources of the FRI class are 3C 120 (Walker, Benson, & Unwin 1987; Benson et al. 1988) and M87 (Reid et al. 1989) which show one-sided jets. Both can be mapped with Mark II. A few more objects of intermediate luminosity have recently been observed with the more sensitive Mark III technique, with the goal of comparing their parsec-scale morphology with that of the more luminous objects (Giovannini et al. 1992).

We present here a 5 GHz VLBI map of 3C 338 (R.A.$_{B1950}$ = $16^h26^m55^s.4$, Decl.$_{B1950}$ = 39°39′36″), which represents the first case of a radio galaxy showing a emission on both sides of a milliarcsecond (mas) core. Preliminary images were presented by Giovannini et al. (1993). This radio galaxy has a total radio luminosity at 408 MHz of 1.78×10^{25} W Hz^{-1} sr^{-1}, and is classified as a FRI source. 3C 338 has the steepest radio spectrum at centimeter wavelengths of any 3CR source except 3C 318.1. It is associated with the multiple-nuclei cD galaxy NGC 6166 ($z = 0.031$), located at the center of the cooling flow cluster of galaxies A2199. We also present new VLA observations at 5 and 8.4 GHz.

3C 338 belongs to a complete sample of radio galaxies selected for VLBI observations (Giovannini, Feretti, & Comoretto 1990), to investigate the milliarcsec-scale properties of a sample covering a large range of radio luminosity and to study the connection of milliarcsec with arcsec structure. The observations presented here were obtained at 5 GHz with the European VLBI Network (EVN) and United States VLBI Network (USVN) arrays, achieving a resolution of 1 mas. Throughout, we use $H_0 = 100$ km s^{-1} Mpc^{-1}: using 91 Mpc as the distance of 3C 338, 1 mas corresponds to 0.47 pc.

2. OBSERVATIONS AND DATA REDUCTION

2.1. *VLBI*

We observed 3C 338 at 5 GHz on 1989 September 25, for 7 hr, with a EVN + USVN array consisting of the following nine radio telescopes: Bonn, Jodrell Bank MK2, Onsala, Westerbork Synthesis Radio Telescope tied array (WSRT), Green Bank 140-foot, Haystack, Owens Valley 130-foot, Very Long Baseline Array (VLBA)-Pie Town, and Very Large Array (VLA). The full VLA in the standard C configuration was available during the observations and was *phased up* with observations of DA 406 every 30 minutes. Data were recorded with the Mark III recording system (Alef 1989), with a bandwith of 28 MHz (Mode B). In mode B, each tape records data for 28 minutes, followed by a 7 minute data gap while the tapes are changed. The resulting *u-v* coverage, shown in Figure 1, ranges from ~0.6 to ~140 Mλ, the shortest spacings being provided by the interferometer Pie Town-VLA. The clumpy nature of the *u-v* coverage, partially due to observing failures of 1–2 hr at Bonn and Jodrell Bank telescopes, arises essentially by the nonuniform distribution of telescopes. At the time of the observations, no other antennas of the EVN and USVN were equipped with the Mark III recording system. We used as a calibrator source 1739+522, whose flux density was 1.77 Jy, measured during the observations at Bonn, WSRT, and Owens Valley. The uncertainty of the absolute flux density calibration of the data is about 5%–10%, as usual for VLBI.

The data were correlated in Bonn. After the fringe searching and data correlation, fringe fitting was performed by means of the program FRNGE (Alef 1989). The output visibilities were then written in FITS format and transported into the Caltech

[1] Istituto di Radioastronomia del CNR, Via Irnerio 46, I-40126 Bologna, Italy.
[2] Dipartimento di Astronomia dell'Universitá, Bologna, Italy.
[3] Osservatorio Astrofisico di Arcetri, L.go E. Fermi 5, I-50126 Firenze, Italy.
[4] Infrared Processing and Analysis Center, California Institute of Technology, M/S 100-22, Pasadena, CA 91125.

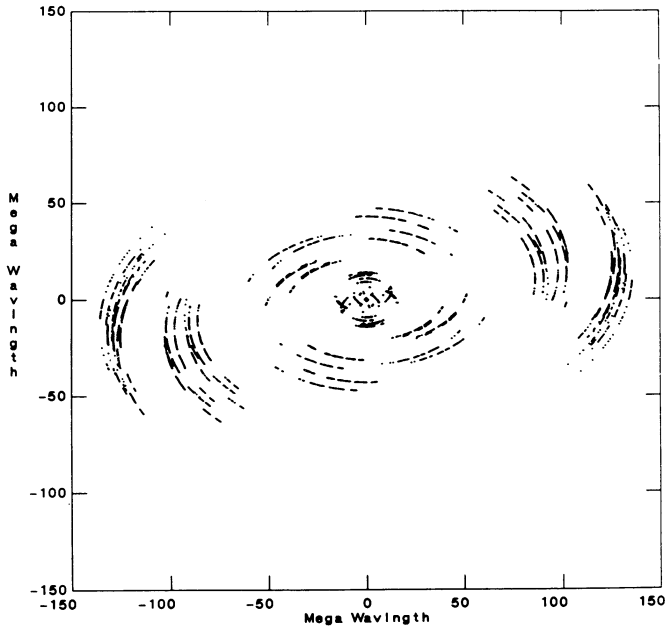

FIG. 1.—Spacings of the observation in the *u-v* plane

VLBI package (CIT; Pearson 1991) where they were converted to MRG format. As a first step, the data were interactively edited to delete bad points. The default values of the antenna gains were checked through the calibrator 1739+522. This check was made on the EVN and USVN baselines separately to overcome the possibility that 1739+522 was resolved on the transatlantic baselines. Corrections to the antenna gains were of order of 5%. The calibrated data (see Fig. 2) were then self-calibrated and mapped using two packages, CIT and the NRAO Astronomical Image Processing System (AIPS). These two packages use basically the same algorithms, however they differ in the effective use of weighting of the data, in the interpolation function used in gridding and in the interactive control of the CLEANing procedure.

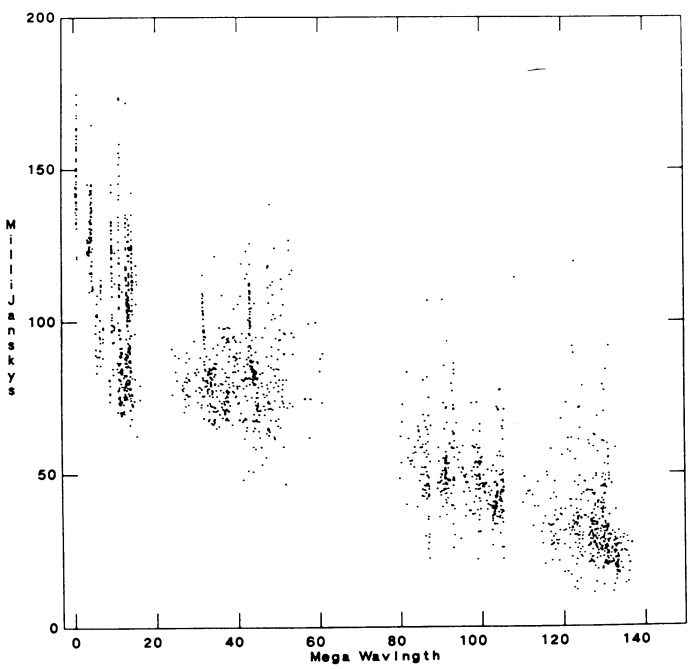

FIG. 2.—Visibility amplitudes vs. projected baseline

2.1.1. *Mapping with the CIT Package*

In the CIT package, we fitted circular Gaussian models to the data by means of the program MODELFIT, which uses both amplitudes and closure phases of the input visibilities. We first tried to constrain components to be on one side of the most compact component, but the fits to the visibility amplitudes and to the closure phases were not satisfactory. The agreement factor (defined as the reduced χ^2) between the model and data of the closure phases improved from 3 to 2.4 when the model was permitted to have extended emission on both sides. We show in Figure 3 the closure phases of three significant triangles, showing the one-sided and two-sided model fits, respectively.

Our best model consisted of five Gaussians: a bright extended component containing ~45% of the flux, and the others located in a double-sided structure with respect to the bright one, for a total extent of ~20 mas. This model was used for the self-calibration of phases.

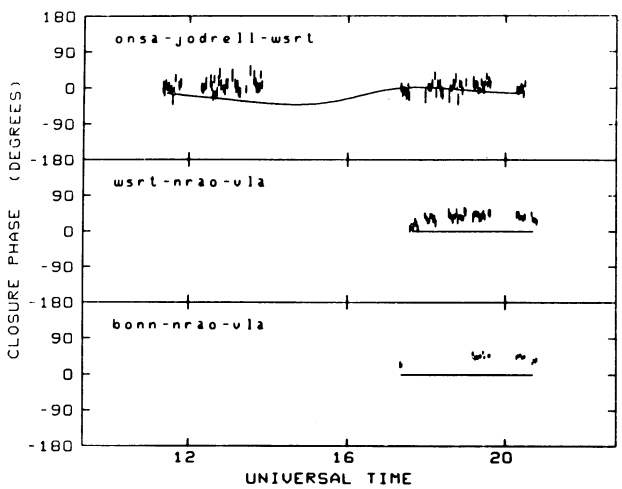

FIG. 3*a*

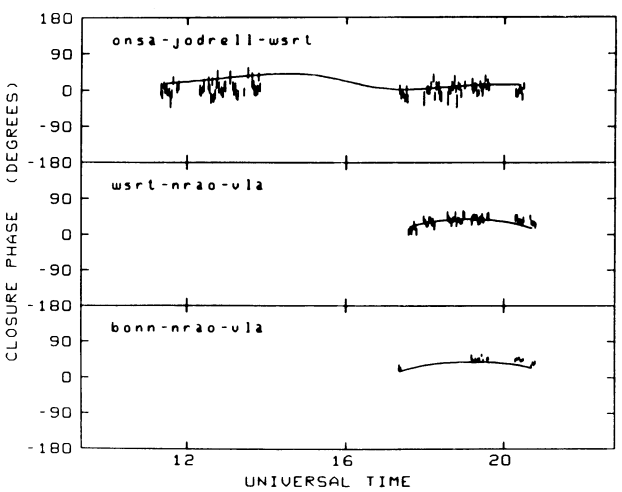

FIG. 3*b*

FIG. 3.—Plot of the original closure phases of three triangles. Continuous lines represent (*a*) one-sided source model and (*b*) two-sided source model.

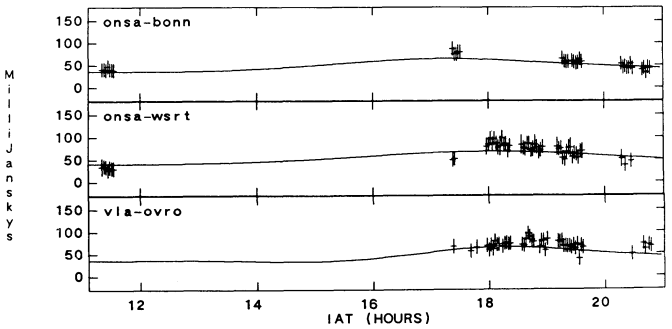

FIG. 4.—Visibility amplitudes derived from the CLEAN components of the final map (*lines*) and actual data (*crosses*) for relevant baselines, after subtraction of the strong central component.

Then the hybrid mapping procedure was started (Readhead & Wilkinson 1978). Initially, phase self-calibration was applied in the program AMPHI to the longest baselines by restricting the UV range to values greater than 60 Mλ, then all the baselines were included in the self-calibration. Amplitude self-calibration with averaging time of 1 hr was allowed twice, at the very end of the hybrid mapping cycle. The final map has a noise level of 0.4 mJy beam^{-1}.

A parallel attempt was made to make a good hybrid map by permitting CLEAN components only in a box containing the bright source and a one-sided structure, but no convergence was reached. The map was always very noisy ($\sim$1.5 mJy beam^{-1}) and the closure phase agreement factor did not improve. This procedure was tried with boxes on either side of the strongest feature, with the same result. The hybrid mapping procedure converged only when emission on both sides of the strongest feature was permitted.

2.1.2. *Mapping with AIPS*

MRG format data were transformed back to FITS format, then transported into AIPS. The phases of the original UV data were self-calibrated using a point source as a starting model. Hybrid mapping iterations were performed by means of the programs MX and CALIB. We applied phase corrections using those features with brightness exceeding 5–7 times the rms noise level in the map, measured far from the map center. At each step the baseline range was restricted to long spacings with visibility amplitudes below the total flux density of the model. When a satisfactory agreement between the data and the model was reached, and no further improvement was obtained with the phase self-calibration only, we allowed amplitude self-calibration with a 2 hr integration time, still with a UV-range restriction based on the flux density present in the model. The final UV-data set was used to produce maps with two different deconvolution algorithms: CLEAN and Maximum Entropy Method (MEM). The CLEAN map was obtained by first permitting CLEANing in a box around the brightest features, and then allowing CLEANing entire over the field. A low CLEAN loop-gain (=0.08) was used, to avoid producing artificial knots, which might arise from the clumpy nature of the *u-v* coverage. The resulting image has an rms of 0.35 mJy beam^{-1}. Since the source is dominated by the central feature, the comparison between the visibilities and the model implied by this image was performed after subtracting in the (*u*, *v*) plane two pointlike components, located at the peak of radio emission, separated by 0.3 mas in R.A., with total flux of 48 mJy. The data and model amplitudes relative to three baselines, showing some structure, are displayed in Figure 4. The MEM was applied with the AIPS task VTESS after subtraction of a point source of 30 mJy at the center. This method was used to check that the knots present in the CLEAN map were not artifacts of the CLEAN algorithm, and to enhance possible low surface brightness features. The rms noise in this image is 0.4 mJy beam^{-1}.

Using AIPS, as we did with the CIT package, we repeated the whole reduction procedure, forcing the CLEAN on a one-sided box to see if a source with asymmetric structure is still a good representation of the data. The final map had a much higher rms noise than the map with two-sided structure and there was always some residual flux present on the opposite side of the box.

From the previously described reduction procedures, we conclude that the two-sided structure is real. We also note that the brightness distribution on the two sides is anticorrelated with respect to distance from the central source (see the discussion about alternating, intrinsically one-sided jet in § 4). This is a strong evidence that the two-sided features are not a result of spurious symmetrization in the image-reconstruction process.[5]

The CIT map, the AIPS-CLEAN map, and the AIPS-MEM map agree in the principal features. Differences in the details of the low brightness structure are at levels less than 3 σ. We show here (Fig. 5) the AIPS map, obtained with the CLEAN

[5] We thank an anonymous referee for pointing out this further indication of the reality of the observed structure.

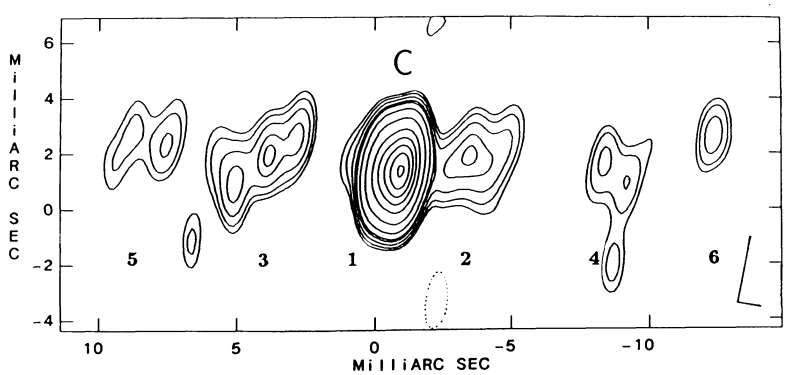

FIG. 5.—VLBI contour map of 3C 338 at the resolution of 2.4 × 0.9 mas (p.a. = −10°). The half power beamwidth is represented, in this and the other maps, by the L-shaped sign in the lower right-hand corner. The rms noise is 0.35 mJy beam^{-1}. Contours are −1, 1, 1.3, 1.8, 2.5, 3, 5, 10, 20, 30, 40, 50, 60 mJy beam^{-1}. The numbers label a possible sequence of alternate blob ejection (see § 4).

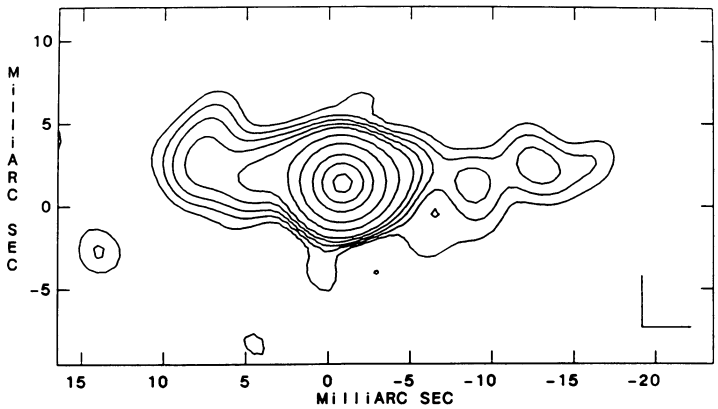

FIG. 6.—VLBI contour map of 3C 338 smoothed at the resolution of 3.2 mas. The rms noise is 0.4 mJy beam^{-1}. Contours are -1.2, 1.2, 1.8, 2.5, 3.5, 5, 10, 20, 40, 60, 80 mJy beam^{-1}.

technique. Its half-power beamwidth is 2.4×0.9 mas (p.a. $= -10°$).

To improve the sensitivity to extended emission, we also produced a low-resolution map (Fig. 6), using only the u-v spacings up to 55 Mλ. The half-power beamwidth of the circular synthesized beam is 3.2 mas, and the rms noise level is 0.4 mJy beam^{-1}.

2.2. *VLA*

We obtained VLA data with the A array at 5 and 8.4 GHz with the goals of analyzing the subarcsecond structure, searching for the existence of jets, and measuring the core flux density and spectrum. Observations at the two frequencies, respectively, of 30 and 15 minutes duration, took place on 1990 April 2, with a bandwidth of 50 MHz. The data were reduced in AIPS according to the standard procedure for synthesis imaging (e.g., Sramek & Schwab 1989; Cornwell & Braun 1989). The 5 GHz map has an angular resolution of 0.″4 (HPBW) and an rms noise level of 0.04 mJy beam^{-1}, while the 3.6 cm map has an angular resolution of 0.″25 and an rms of 0.08 mJy beam^{-1}.

3. RESULTS

3.1. *VLBI*

The full-resolution VLBI map is shown in Figure 5. The radio emission is dominated by a bright feature (C in the figure), slightly extended in p.a. 90°, which contains $\sim$70% of the total VLBI flux density. On both sides of the brightest feature, "knotty" radio emission is detected, with the main structures along p.a. 90° and $-90°$. The maximum strength of the "knotty" structures is about 1/20 that of the central peak. They extend $\sim$10 and $\sim$12 mas to the east and west, respectively. Their structures may be marginally affected by sidelobes of the synthesized beam, however, the knots are not colocated with prominent sidelobes. The structure within 5–7 mas from the strong central source is on both sides at the 10 σ level, while the outermost blobs are at 5 σ. The total (projected) linear extent of the structure is $\sim$10 pc. The total flux density in this map is 133 mJy, which corresponds to $\sim$90% of the flux density of the VLA arcsec core, measured in 1989 April (154 mJy; J. P. Ge 1990, private communication). The "missing flux" could occur on the shorter baselines (see Fig. 2) that our observations have, or it could simply reflect the accuracy of the calibration. Since the "missing flux" is only a small fraction of the total flux density, its true nature does not change the general parsec-scale morphology.

The total flux densities of the eastern and western knotty regions, obtained by integration over the brightness distribution, are 20 ± 1 and 21 ± 1 mJy, respectively. The flux density of the "C" component is 92 mJy.

In the low-resolution VLBI map the low brightness structure is more clearly visible (Fig. 6). It is still elongated in p.a. $\sim 90°$ and $-90°$, with a total extent of about 12 pc. The eastern side is shorter and brighter than the western one. No extended emission was found to be present around the jets.

3.2. *VLA*

In the high-resolution VLA map, obtained by us with the A configuration at 5 GHz, the structure is characterized by two weak, almost completely resolved *spots* of radio emission, located on both sides of the unresolved core. The structure is aligned within 5° of the VLBI structure. The peak flux densities of the eastern and western spots are 1.9 and 1.0 mJy, respectively. A map convolved to the resolution of 0.″7 is shown in Figure 7. Here the spot flux densities increase to 3.4 and 2.5 mJy, respectively, confirming that they are resolved. No jet is seen between the core and each spot. The core flux density is 168 mJy, i.e., significantly higher than that measured by J. P. Ge (see above) about a year earlier. This implies that the core is variable, as confirmed by inspection of other data from the literature (see § 4).

In the VLA map at 3.6 cm (A configuration, not shown here), the structure is completely resolved out, and only the compact

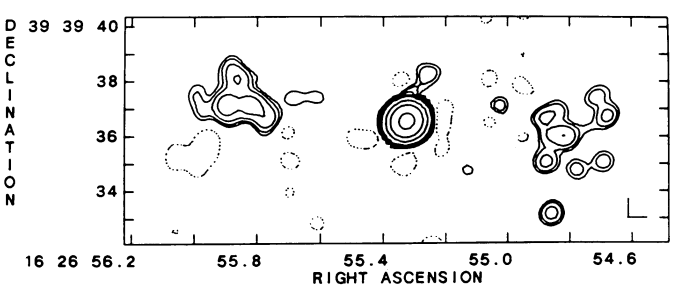

FIG. 7.—VLA contour map of 3C 338 with the angular resolution of 0.″7. The rms noise is 0.035 mJy beam^{-1}. Contours are -0.1, 0.1, 0.15, 0.25, 0.5, 1, 5, 20, 100 mJy beam^{-1}.

core is detected. These data are, however, very important for the measurement of the core flux density and the determination of the core spectrum. The core flux density is 143 mJy at 8.4 GHz, yielding a spectral index[6] $\alpha = 0.3$ between 5 and 8.4 GHz.

3.3. *Core Location*

The moderately flat spectrum of the arcsec core is consistent with the presence of a compact core and a structure with steeper spectrum. This is confirmed by the VLBI map, where most of the structure is resolved. Since 90% of the VLA core flux density is present in the VLBI map, if we assume that the parsec-scale jet has a spectral index ~ 0.5, the flat-spectrum core has to be coincident with the structure "C", or part of it. On the other hand, if the flat spectrum core were identified with a faint knot, all the parsec-scale structure should have a spectrum $= 0.3$ to justify the value found with the VLA observations. We conclude that it is very unlikely that the radio core coincides with one of the weak VLBI knots. The strong central radio source, which is also the most compact, is the most reasonable location of the active core, and the eastern and western radio emissions come from two-sided jets.

4. DISCUSSION

Based on its radio luminosity, the radio galaxy 3C 338 is classified as FRI, but its morphology is quite unusual for FRI sources. It exhibits a compact core, coincident with the brightest nucleus of the multiple optical system, and an elongated (jet + lobelike) feature, shifted a few arcseconds to the south with respect to the core (Burns, Schwendeman, & White 1983). One interpretation of its morphology is that it is a "normal" head-tail galaxy which we observe moving away from us through the cluster medium. The spectrum of the last feature is very steep ($\alpha = 1.69$ and $\alpha = 1.58$ respectively for the "jet" and for the "lobe", Burns et al. 1983; J. P. Ge 1990, private communication). In Figure 8 we present a composite map showing the source structure at different resolutions. It is evident that the parsec-scale structure is strictly connected to the kiloparsec-scale one, and symmetry holds in this source over all distance scales.

Other jets with two-sided milliarcsec structure have been reported in the literature (see Spencer & Akujor 1992, for a review), but generally the counterjet is weaker and shorter than the jet, leading to a basically asymmetric structure. In 3C 236 (Barthel et al. 1985; Schilizzi et al. 1988) the jet and counterjet are symmetric at 18 cm, but the overall structure at 18 cm and the jets at 6 cm are asymmetric.

3C 338 is the first case where the milliarcsec-scale jets are very similar in strength and length. This implies that Doppler boosting is not important, leading to the conclusion that either the source lies in the plane of sky or the jets in this object are nonrelativistic. At present, no estimate of the jet velocity can be done. A source orientation in the plane of the sky is supported by the symmetry detected on the large scale. The only possible asymmetry in this source could be seen at the level of the strongest VLBI component itself, which is resolved, and is therefore likely to contain, besides the unresolved core, the beginning of the jet(s). Higher resolution observations are necessary to separate in the "C" feature the true core from the jet emission.

[6] $S(\nu) \propto \nu^{-\alpha}$.

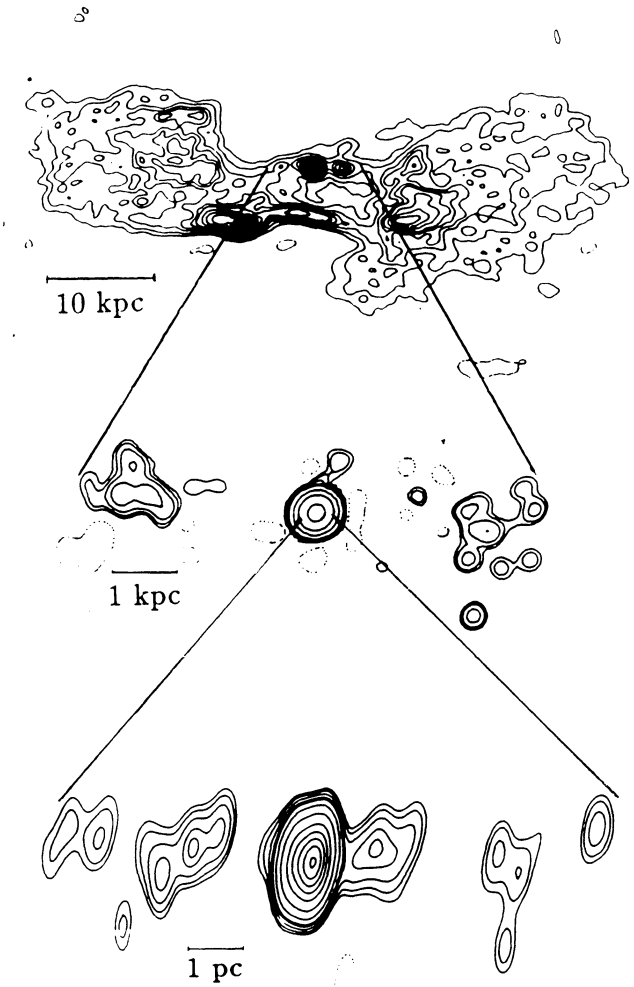

FIG. 8.—Composite map showing the structure of 3C 338 with different resolutions. The linear scale is indicated on each map. The large-scale map is taken from Fanti et al. (1986).

From the symmetric structure found at the parsec scale, where the ratio of jet flux densities is $\sim 1:1.1$, we can constrain the product $\beta \cos\theta$, where β is the ratio of the jet flow velocity to the speed of light and θ is the angle to the line of sight. Assuming a jet spectral index of 0.5, we obtain $\beta \cos\theta \lesssim 0.019$, which implies that the angle to the line of sight is $\geq 88°$, for any value of $\beta \gtrsim 0.5$.

A second attracting possibility is that the jet is intrinsically one-sided and alternately feeds energy into the opposite lobes. This might be suggested by the observed parsec structure, which, when mirrored with respect to the peak, fills in the gaps nicely. In this case, a possible sequence of alternate blob ejections would be that indicated by the numbering given in Figure 5 and the period of blob ejection would be about $3/(\beta \sin\theta)$ years. The relative strength of supposedly successive blobs would indicate that their flux density fades very quickly after the emission (the flux ratio of blob 1 to blob 2 is > 10) and then remains more or less constant.

The lack of visible jets in the arcsec-scale structure is quite surprising. The absence of a jet in the VLA map of Figure 7 indicates that the jets emanating from the nucleus are disrupted within about 100 pc and this is likely to be due to the strong interaction between the energy flow and the environ-

ment. Since this radio galaxy is at the center of a cooling flow, the effect of a cooling flow on jets may be dramatic. We note that the radio galaxy 3C 84, lying at the center of the Perseus cluster, has jets that disrupt very close to the nucleus (Venturi et al. 1993).

A search among published data at 5 GHz has revealed that the arcsec core radio emission is variable: 105 mJy in 1980.34 (Burns et al. 1983), 154 mJy in 1989.26 (J. P. Ge 1990, private communication), 168 mJy in 1990.25 (this paper). Also the flux density detected with VLBI has shown variability: 100 mJy in 1985.79 (Giovannini et al. 1990), 133 mJy in 1989.73 (this paper). Owing to its variability, this source is a candidate for change of structure. Unfortunately, the sensitivity and UV coverage in the data presented by Giovannini et al. (1990) were not enough to produce an unambiguous map.

In many cases, variability has been found to be related to superluminal motion in the VLBI structure. Using standard formulae for the superluminal motion (Pearson & Zensus 1987), we derive that the proper motion in this source could be of order 0.36 to 0.67 mas yr^{-1}, with $\beta = 0.5$ to 0.9, respectively. Therefore, a 2 to 4 yr monitoring program should allow us to better constrain the intrinsic speed of the flow.

The existence of a twin-jet source like 3C 338 on the VLBI scale is not a fatal blow to the unified scheme in which the FRI radio galaxies are the parent population of BL Lac objects (Blandford & Rees 1978; Padovani & Urry 1990). In fact, 3C 338 can be nicely interpreted as being on the plane of the sky and therefore not affected by any orientation bias. If the distribution of the orientation angles of radio galaxies with respect to the line of sight is uniform, we expect $\sim 5\%$ of the galaxies in a sample selected at low frequencies (e.g., 408 MHz) to be at $\theta \geq 88|^{\circ}$. A further reduction in the fraction of sources is expected if sources are selected preferentially toward the line of sight. In our sample of 27 sources (Giovannini et al. 1990), we expect only one source oriented at $\theta \geq |88|^{\circ}$. If many other cases of two-sided VLBI jets were found in flux-limited samples selected at low frequencies, the unification schemes (see e.g., Orr & Browne 1982) would be in trouble.

5. CONCLUSIONS

We have presented the milliarcsec and arcsec scale structure of the FRI radio galaxy 3C 338. This radio source represents the first case of symmetric, two-sided structure in a radio galaxy on parsec scales. The reality of this structure has been tested with different reduction procedures, which should exclude any artificial features of the same brightness. New data at different frequencies are being obtained to confirm this structure and to study the physical conditions of this source. The results of this paper can be summarized as follows:

1. The main characteristics of the milliarcsec structure of 3C 338 are a strong central feature containing 70% of the total VLBI flux density which is slightly asymmetric; and two jets, located on both side of the strongest feature, with very similar brightness and extent.

2. The arcsec structure, mapped with the VLA at 0".4 resolution, consists of a compact core and two symmetric spots $\sim 6''$ (~ 3 kpc) of the core, with no jets visible in between. The arcsec core contains 10% more flux than the VLBI map.

3. Symmetry holds on both the milliarcsec- and arcsec-scale structures, which are aligned with each other within 5°.

4. The milliarcsec structure can be interpreted as originating from a core plus two-sided relativistic jets which are oriented approximately on the plane of the sky. Alternatively, a flip-flop model can nicely explain the structure. The jets disrupt within ~ 100 pc of the nucleus, given that no jets are visible in the A-array VLA map.

5. The radio emission of the arcsec core, as well as that detected in the VLBI map, has been found to be variable, with an increase of at least 60% in 10 yr. Therefore, this source is a good candidate for changes in its parsec-scale structure.

We thank T. J. Pearson for help and discussions on the reduction procedure. Thanks are due to many colleagues of the Istituto di Radioastronomia for useful comments on the manuscript, and to N. Primavera for drawing the figures.

L. F. and G. G. wish to thank the NRAO, Socorro (NM), for the hospitality during part of this work. They acknowledge financial support from CNR-NATO fellowships and Italian MURST.

We wish to thank the observatories of the European and US VLBI networks for their contribution to this experiment. We also thank D. Graham and the Mark III-correlator staff in Bonn for the careful correlation of these data.

REFERENCES

Alef, W. 1989, in Very Long Baseline Interferometry, ed. M. Felli & R. E. Spencer (Dordrecht: Kluwer), 97
Barthel, P. D., Schilizzi, R. T., Miley, G. K., Jägers, W. J., & Strom, R. G. 1985, A&A, 148, 243
Benson, J. M., Walker, R. C., Unwin, S. C., Muxlow, T. W. B., Wilkinson, P. N., Booth, R. S., Pilbratt, G., & Simon, R. S. 1988, ApJ, 334, 560
Blandford, R., & Rees, M. 1978, in Proc. Pittsburgh Conf. on BL Lac Objects, ed. A. N. Wolfe (Pittsburgh: Univ. Pittsburgh), 238
Burns, J. O., Schwendeman, E., & White, R. A. 1983, ApJ, 271, 575
Cohen, M. H., et al. 1975, ApJ, 201, 249
Cornwell, T., & Braun, R. 1989, in Synthesis Imaging in Radio Astronomy, ed. R. A. Perley, F. R. Schwab, & A. H. Bridle (ASP Conf. Ser., 6), 167
Fanaroff, B. L., & Riley, J. M. 1974, MNRAS, 167, 31P
Fanti, C., Fanti, R., De Ruiter, H. R., & Parma, P. 1986, A&AS, 65, 145
Giovannini, G., Comoretto, G., Feretti, L., Marcaide, J., Venturi, T., Vermeulen, R., & Wehrle, A. E. 1992, Proc. of the Heidelberg Conference on Physics of Active Galactic Nuclei, ed. W. J. Duschl & S. J. Wagner (Berlin: Springer), 561
Giovannini, G., Feretti, L., & Comoretto, G., 1990, ApJ, 358, 159
Giovannini, G., Venturi, T., Feretti, L., Comoretto, G., & Wehrle, A. E. 1993, Proc. Ringberg Workshop on Jets in Extragalactic Radio Sources, in press
Orr, M. J. L., & Browne, I. W. A. 1982, MNRAS, 200, 1067
Padovani, P., & Urry, C. M. 1990, ApJ, 356, 75
Pearson, T. J. 1991, BAAS, 23, 991
Pearson, T. J., & Zensus, A. 1987, in Superluminal Radio Sources, ed. T. J. Pearson & A. Zensus (Cambridge: Cambridge Univ. Press), 1
Readhead, A. C. S., & Wilkinson, P. N. W. 1978, ApJ, 223, 25
Reid, M. J., Biretta, J. A., Junor, W., Muxlow, T. W. B., & Spencer, R. E. 1989, ApJ, 336, 112
Schilizzi, R. T., Skillman, E. D., Miley, G. K., Barthel, P. D., Benson, J. M., & Muxlow, T. W. B. 1988, in IAU Symp 129, The Impact of VLBI on Astrophysics and Geophysics, ed. M. J. Reid & J. M. Moran (Dordrecht: Kluwer), 127
Spencer, R. E., & Akujor, C. E. 1992, in Extragalactic Radio Sources—From Beams to Jets, ed. J. Roland, H. Sol, & G. Pellettier (Cambridge: Cambridge Univ. Press), 119
Sramek, R. A., & Schwab, F. R. 1989, in Synthesis Imaging in Radio Astronomy, ed. R. A. Perley, F. R. Schwab, & A. H. Bridle (ASP Conf. Ser., 6), 117
Venturi, T., Readhead, A. C. S., Marr, J. M., & Backer, D. C. 1993, ApJ, in press
Walker, R. C., Benson, J. M., & Unwin, S. C. 1987, ApJ, 316, 546